

## Research Article

# Klotho Ameliorates Podocyte Injury through Targeting TRPC6 Channel in Diabetic Nephropathy

Xingmei Yao,<sup>1</sup> Hengjiang Guo,<sup>2</sup> Mengyao Sun,<sup>1</sup> Sixuan Meng,<sup>1</sup> Bingbing Zhu,<sup>1</sup> Ji Fang,<sup>1</sup> Jiebo Huang,<sup>1</sup> Hao Wang<sup>ID</sup>,<sup>1</sup> and Lina Xing<sup>ID</sup><sup>1</sup>

<sup>1</sup>Department of Nephrology, Putuo Hospital, Shanghai University of Traditional Chinese Medicine, Shanghai 200062, China

<sup>2</sup>Department of Anesthesiology, Shanghai Children's Hospital, Shanghai Jiao Tong University, Shanghai 200062, China

Correspondence should be addressed to Hao Wang; wang402hao@163.com and Lina Xing; 13918035850@163.com

Received 18 October 2021; Accepted 14 March 2022; Published 18 April 2022

Academic Editor: Saheed Sabiu

Copyright © 2022 Xingmei Yao et al. This is an open access article distributed under the Creative Commons Attribution License, which permits unrestricted use, distribution, and reproduction in any medium, provided the original work is properly cited.

Podocyte damage is vital for the etiopathogenesis of diabetic nephropathy (DN). Klotho (KL), a multifunctional protein, has been demonstrated to have renoprotective effects; nevertheless, the mechanism for protective effect has not been completely elucidated. Transient receptor potential cation channel subfamily C, member 6 (TRPC6), a potential target of KL, is implicated in glomerular pathophysiology. Here, we sought to determine whether KL could protect against podocyte injury through inhibiting TRPC6 in DN. We found that high glucose (HG) triggered podocyte injury as manifested by actin cytoskeleton damage along with the downregulation of KL and Synaptopodin and the upregulation of TRPC6. KL overexpression reversed HG-induced podocytes injury, whereas cotreatment with TRPC6 activator flufenamic acid (FFA) significantly abrogated the beneficial effects conferred by KL. Moreover, KL knockdown in podocytes resulted in actin cytoskeleton impairment, decreased Synaptopodin expression, and increased TRPC6 expression. In *db/db* mice, KL overexpression inhibited TRPC6 expression and attenuated diabetes-induced podocyte injury, which was accompanied by decreased albuminuria and ameliorated glomerulosclerosis. Our data provided novel mechanistic insights for KL against DN and highlighted TRPC6 as a new target for KL in podocytes to prevent DN.

## 1. Introduction

With the growing incidence and prevalence of diabetes mellitus (DM) around the world, diabetic nephropathy (DN), a severe complicating disease of DM, has been the primary cause of end-stage renal disease (ESRD) [1, 2]. Clinically, DN is characterized by progressive proteinuria which is most closely related to podocyte injury [3]. Podocytes are greatly specialised cells with intricate cell structure in glomeruli whose dysfunction results in deterioration of glomerulus filtration barrier and proteinuria [4, 5]. The precise function of podocytes relies on the proper organization of the actin cytoskeleton, and actin cytoskeletal rearrangement is a common pathological process for glomerulus diseases [4, 6]. However, the mechanisms underlying podocyte actin cytoskeleton rearrangement have not been fully clarified.

Klotho (KL), originally identified as an antiaging gene, encodes a single-pass transmembrane protein with high abundance in renal and cerebral tissues [7]. There are two distinct forms of KL. The membrane-bound form is a cofactor for fibroblast growth factor 23 (FGF23) and plays a critical role in modulating phosphate homeostasis. The secreted soluble form acts as a hormone with antioxidative stress, anti-inflammatory, and antisenescent properties [8]. Recently, the renoprotective effect of KL has aroused increasing interest. Reduced kidney KL expression was identified in both humans and animals with various renal diseases [9]. Additionally, the decrease in plasma KL has been suggested to be an indicator for DN progression in type 2 diabetic patients [10]. A growing number of evidences revealed that KL overexpression confers renoprotection. Haruna et al. [11] confirmed KL overexpression alleviated not only tubulointerstitial damage but also

glomerulosclerosis. Wang et al. [12] displayed that KL overexpression weakened DN through ameliorating HG-triggered damage of glomerular endothelial cells. We and others also proved KL-conferred podocyte protection in DN [13–15]. Nevertheless, the molecular mechanism by which KL protects against podocyte injury in DN warrants further study.

The canonical transient receptor potential channel (TRPC) 6, a member of the TRPC family of nonselective  $\text{Ca}^{2+}$ -permeable cation channels, has been implicated in the pathogenesis of glomerular diseases [16]. Gain-of-function mutations in TRPC6 cause hereditary familial focal segmental glomerulosclerosis [17, 18]. Moreover, TRPC6 is upregulated in several proteinuric kidney diseases including DN [19–21], which may be relevant to podocyte damage because Angiotensin II, reactive oxygen species (ROS), and other factors in the setting of DN directly activate TRPC6 activity and result in drastic increases in  $\text{Ca}^{2+}$  influx, causing podocyte actin cytoskeleton dynamics, hypertrophy, and foot process effacement [22–25]. Moreover, nonspecific overexpression of wide-type TRPC6 in mice leads to transient proteinuria [20], while TRPC6 deficiency protects podocytes and kidney function during the development of DN [26, 27]. These findings suggested that TRPC6 is an attractive treatment target of DN. Recently, the findings that KL exerts cardioprotection via the downregulation of TRPC6 pathways in the mouse heart [28] and that KL might mitigate proteinuria via targeting TRPC6 pathways in podocytes [29] raise the possibility that TRPC6 is a downstream target of KL in podocytes in DN. For that reason, herein, our study tested whether KL alleviated DN through inhibiting TRPC6 channel in HG-activated podocytes *in vitro* and diabetic *db/db* murine model *in vivo*.

## 2. Materials and Methods

**2.1. Cell Culture and Treatment.** The immortalized human podocyte cell line, offered by Prof. Niansong Wang (Shanghai Sixth People's Hospital, China), was cultured as depicted previously [30]. Briefly, undifferentiated podocytes were maintained at 33°C (the permissive temperature) in Roswell Park Memorial Institute 1640 (RPMI 1640) added with 10% Fetal Bovine Serum (FBS) and 1% insulin-transferrin-selenium (ITS, all from Thermo Fisher Scientific). For differentiation, cells were preserved under 37°C in the absence of ITS for 7 to 10 days to differentiate into mature podocytes. Mature podocytes were subjected to serum starvation in medium with 1% FBS prior to the exposure to 5 mM D-glucose (low glucose, LG) ( ) or 30 mM D-glucose (HG) medium. For KL overexpression experiment, a recombinant adenovirus vector involving murine KL full-length cDNA (Ad-KL) and the NC adenoviral vector involving green fluorescence protein (Ad-NC, CMV-MCS-SV40-EGFP) were purchased from Genechem (Shanghai, China). The differentiated podocytes were subjected to infection with Ad-KL or Ad-NC at a multiplicity of infection (MOI) of 20 for 24 h prior to cultivation with HG with/without 100  $\mu\text{M}$  TRPC6 activator flufenamic acid (FFA; Sigma-Aldrich, St Louis, MO, USA).

**2.2. Animal Experiment.** Ten week-old male diabetes C57BLKS/J-LepR (*db/db*) mice and littermate *db/m* mice were bought from the Model Animal Research Center of NU (Nanjing, China). All animals were kept under specific-pathogen-free (SPF) conditions under 25°C  $\pm$  1°C and moisture of 50% with a 12 h dark/light period and could eat and drink freely. The mouse experiment was accepted by the Ethical Committee of Putuo Hospital, Shanghai University of Traditional Chinese Medicine and completed as per the NIH guidance for the welfare of Lab animals (No. 8023, revised 1978). *Db/db* animals were stochastically separated into 3 groups ( $n = 6/\text{group}$ ): the DN model group (*db/db* animals), DN+Ad-NC group (*db/db* animals with Ad-NC adenovirus injection), and DN+Ad-KL group (*db/db* mice with Ad-KL adenovirus injection). 50  $\mu\text{l}$  of Ad-NC or Ad-KL adenovirus ( $10^{11}$  PFU/ml) was inoculated into *db/db* animals via tail veins. *Db/m* animals were nondiabetic control group. Urine samples were collected with metabolic cages at d0, d7, d14, and d28 after adenovirus injection. Mouse urine albumin and creatinine contents were identified via commercially available kits (Biovision, Milpitas, CA, USA).

**2.3. Histology.** The collected renal samples were subjected to fixation with 4% paraformaldehyde (PFA), dehydration with ethanol, subjected to paraffin embedment, and sliced into 5  $\mu\text{m}$  slices. Then, the slices were stained with periodic acid Schiff (PAS) for morphological assessment. The mesangial matrix expansion was studied via Image Pro plus 6.0 (Media Cybernetics, America), and the semiquantitative score of glomerulosclerosis was identified via a five-grade approach depicted previously [31].

**2.4. Transmission Electron Microscopy (TEM).** For ultrastructure test, 1 mm<sup>3</sup> pieces of kidney cortex samples were subjected to fixation in 2.5% glutaric dialdehyde in 0.1 M phosphate buffering solution (pH = 7.4), postfixed in 1% osmium tetroxide, treated with dehydration in ethanol, and subjected to Spurr's epoxy resin embedment. Subsequently, ultrathin slices were obtained by ultramicrotome via a diamond cutter, double dyed in lead citrate and uranyl acetate, and studied via a Hitachi H7650 TEM imaging instrument. The width of podocyte foot process was measured and calculated as previously reported [32].

**2.5. Immunofluorescence.** Mouse kidney tissues were frozen in OCT (Thermo Fisher Scientific) and sectioned to 5  $\mu\text{m}$  thickness. The slices were subjected to fixation in prechilled acetone for 600 s under -20°C, blocked in 5% Bovine Serum Albumin (BSA) under RT for 60 min, and incubated at 4°C with the primary antibodies below: anti-KL antibody (Santa Cruz, CA, America), anti-Podocin antibody (Abcam, MA, USA), anti-WT-1 antibody (Abcam, MA, America), and anti-Synaptopodin antibody (Santa Cruz, CA, America). Fluorochrome-conjugated secondary antibodies were acquired from Jackson Immune Research Labs. 4',6-diamidino-2-phenylindole (DAPI) was utilized for nucleus counterstaining.

**2.6. Western Blot Analysis.** Radio-Immunoprecipitation Assay (RIPA) lysis buffer (Beyotime, Shanghai, China) was applied to extract total proteins of kidneys or cultured podocytes. After the determination of protein concentrations, the proteins were separated via sodium dodecyl sulfate polyacrylamide gel electrophoresis (SDS-PAGE). Proteins were transferred onto a polyvinylidene fluoride (PVDF) membrane, blocked with 5% BSA for 60 min, and incubated with primary antibodies overnight at 4°C. After washing, secondary antibodies conjugated with horseradish peroxidase (HRP) were added for 1 h under room temperature. The visualization of the bands was realized via the chemiluminescent approach on GE Healthcare ImageQuant LAS 500 image formation instrument. The OD quantification was studied via Image J program (NIH, MD, America).

**2.7. Quantitative Real-Time PCR (qRT-PCR).** Total RNA was abstracted from podocytes via TRIzol reagent (Invitrogen, CA, USA). 1 µg of overall RNA was converted to cDNAs via a reverse transcript tool (Takara, Dalian, China). qRT-PCR was completed via ABI ViiA™ 7 Real-Time PCR System (Applied Biosystems) using TB Green Premix Ex Taq (Takara, Dalian, China). The PCR mix was incubated under 95°C for 10 min, before 40 cycles of 95°C for 15 sec and 60°C for 1 min. The sequences of primers utilized were presented below: human KL forward: 5'-CAGGACTATCTGCTGATGGACGA-3' and human KL reverse: 5'-CTTTCAAGAGCTCGGCCATC-3' and human β-actin forward: 5'-AAAGGGCAGGCAGGTTCTAT-3' and human β-actin reverse: 5'-CTCCTTAATGTCACGCACGAT-3'. The comparative expression of KL was computed via  $2^{-\Delta\Delta Ct}$  approach with β-actin as the internal control.

**2.8. Phalloidin Staining.** The cells grown on type-1 collagen (Invitrogen, America)-coated cover slips were subjected to fixation in 4% PFA in PBS for 15 min under 37°C, subjected to permeabilization for 5 min in 0.1% Triton X-100 in PBS, blocked for 30 min in PBS with 2% BSA, and incubated with TRITC-phalloidin (Molecular Probes, Invitrogen, Carlsbad, CA) for 20 min under room temperature without light. After washing with PBS, the nucleus was treated with counterstaining with DAPI. Fluorescent pictures were obtained using a laser scanning confocal microscopic device (LEICA DM IRB, Leica, Wetzlar, Germany). The fluorescent intensity of actin fibers was identified via the Image J software (NIH, MD, USA).

**2.9. KL siRNA Transfection.** Differentiated podocytes were subjected to transfection with KL siRNA (siKL) or negative control siRNA (siNC) (GenePharma, Shanghai, China) at an eventual content of 80 nM via Lipofectamine RNAiMAX Transfectional Reagent (Invitrogen, Carlsbad, CA, USA) as per the supplier's specification. The siKL sequence was presented below: sense: 5'-CCGAGAGCAUGAAGAAUAA TT-3' and antisense: 5'-UUAUUCUUCAUGCUCUCGG TT-3'. The siNC sequence was presented below: 5'-UUCU CCGAACGUGUCACGUTT-3' and antisense: 5'-ACGU

GACACGUUCGGAGAATT-3'. The siKL knockdown efficiency was evaluated via WB.

**2.10. Statistics.** Data are described as the mean ± SEM and were analyzed by GraphPad Prism program (GraphPad Software Inc., USA). A two-tailed Student's *t*-test was utilized for comparisons between 2 independent groups, and one-way ANOVA plus Tukey's posttest was employed to compare more independent groups. *P* < 0.05 had significance on statistics.

### 3. Results

**3.1. KL Was Downregulated in HG-Stimulated Podocytes.** Given that hyperglycemia contributes to DN pathogenesis, our study identified the impact of HG on KL expression in podocytes. As shown in Figures 1(a) and 1(b), podocyte cytoskeletons were remarkably disrupted by HG time-dependently as shown by TRITC-conjugated phalloidin staining. HG also reduced the expression levels of KL mRNAs and proteins time-dependently, paralleled by Synaptopodin downregulation (Figures 1(c)-1(e)).

**3.2. Exogenous KL Protected against Podocyte Cytoskeletal Damage Induced by HG.** To test whether the restoration of KL expression could rescue podocyte cytoskeleton disruption induced by HG, we overexpressed KL in HG-cultured podocytes via Ad-KL infection. The efficiency of adenovirus infection was verified by fluorescence examination (Figure 2(a)). As presented by Figures 2(b) and 2(c), KL level in HG-stimulated podocytes was remarkably elevated after infection with Ad-KL, which was accompanied by an elevated expression of Synaptopodin and a decreased expression of TRPC6. TRITC-conjugated phalloidin staining showed that KL overexpression remarkably mitigated the disrupted F-actin stress fiber in podocytes induced by HG (Figures 2(d) and 2(e)).

**3.3. KL Knockdown Damaged Podocyte Cytoskeleton.** To identify the role of KL downregulation in podocyte architecture, our study knocked down KL in cultured podocytes via KL-specific siRNA. KL knockdown resulted in the downregulation of Synaptopodin and the upregulation of TRPC6 (Figures 3(a) and 3(b)). In addition, the stress fiber quantity in podocytes was remarkably decreased via KL knockdown (Figures 3(c) and 3(d)).

**3.4. KL Protected Podocyte Cytoskeleton via Inhibiting TRPC6.** We sought to identify whether KL-conferred cytoskeletal protection was relevant to TRPC6. Western blot showed that cotreatment with TRPC6 activator FFA substantially abolished the upregulation of Synaptopodin expression conferred by KL overexpression in HG-cultured podocytes. Moreover, cotreatment with FFA significantly abrogated the protection of F-actin stress fibers conferred by KL overexpression (Figures 4(c) and 4(d)).

**3.5. KL Was Downregulated in Glomerular Podocytes of Diabetic db/db Mice.** The published transcriptomic data sets in the Nephroseq database showed that KL mRNA

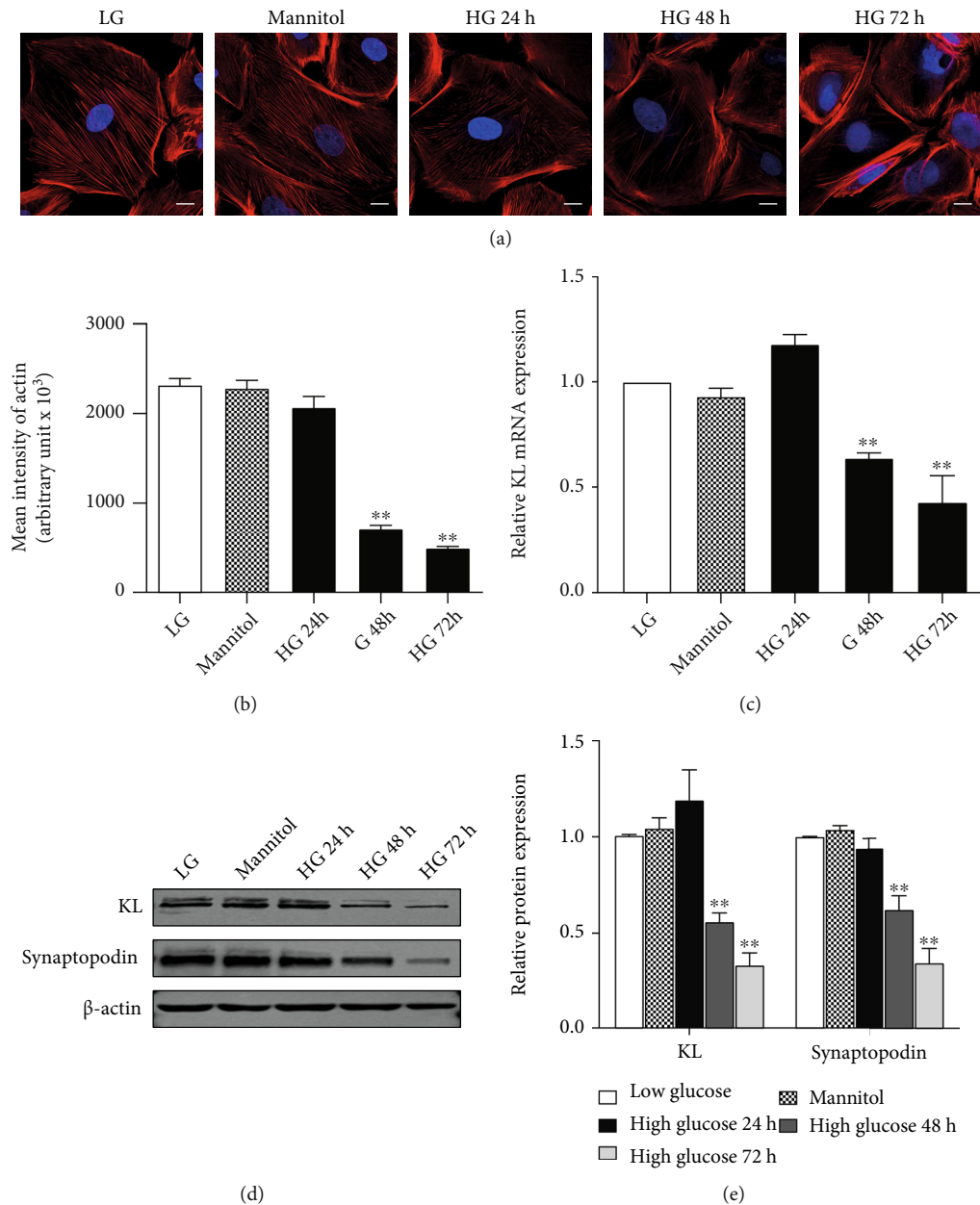


FIGURE 1: HG downregulated KL in podocytes. Podocytes were incubated with HG and collected at the indicated time points. (a) Typical images of phalloidin staining of human podocytes posterior to HG exposure. Scale bars, 10  $\mu$ m. (b) Quantified outcomes in (a). (c) The mRNA expression of KL at various time points. (d) Typical WB and (e) densitometric analyses of KL and Synaptopodin expression at different temporal points.  $n = 3$ . \*\* $P < 0.01$  versus LG group.

expressing was remarkably downregulated in the glomeruli of DN patients in contrast to normal samples (Figure 5(a)). Immunofluorescence staining of KL in mouse renal samples unveiled that KL existed in podocytes, as proved by colocalization of KL with Podocin and Nephlin, the biomarker proteins for podocytes (Figure 5(b)). As shown in Figures 5(c) and 5(d), 16-week-old *db/db* mice displayed massive glomerulus abnormalities, such as glomerular hypertrophy, glomerulosclerosis, and massive podocyte foot process effacement. Immunofluorescence staining revealed that podocyte KL expression was dramatically reduced

accompanied by a reduction of podocyte cell-specific protein Synaptopodin and WT-1. Western blot analysis confirmed that KL and Synaptopodin were downregulated, and TRPC6 was upregulated in the kidney cortex of 16-week-old *db/db* animals (Figures 5(e) and 5(f)).

**3.6. KL Overexpression Attenuated Podocyte Injury in *db/db* Mice.** Finally, we examined the effects of KL overexpression on DN in *db/db* animals. We treated 12-week-old *db/db* animals with Ad-KL or Ad-NC via injection (Figure 6(a)). As presented by Figures 6(b) and 6(c), KL levels in the



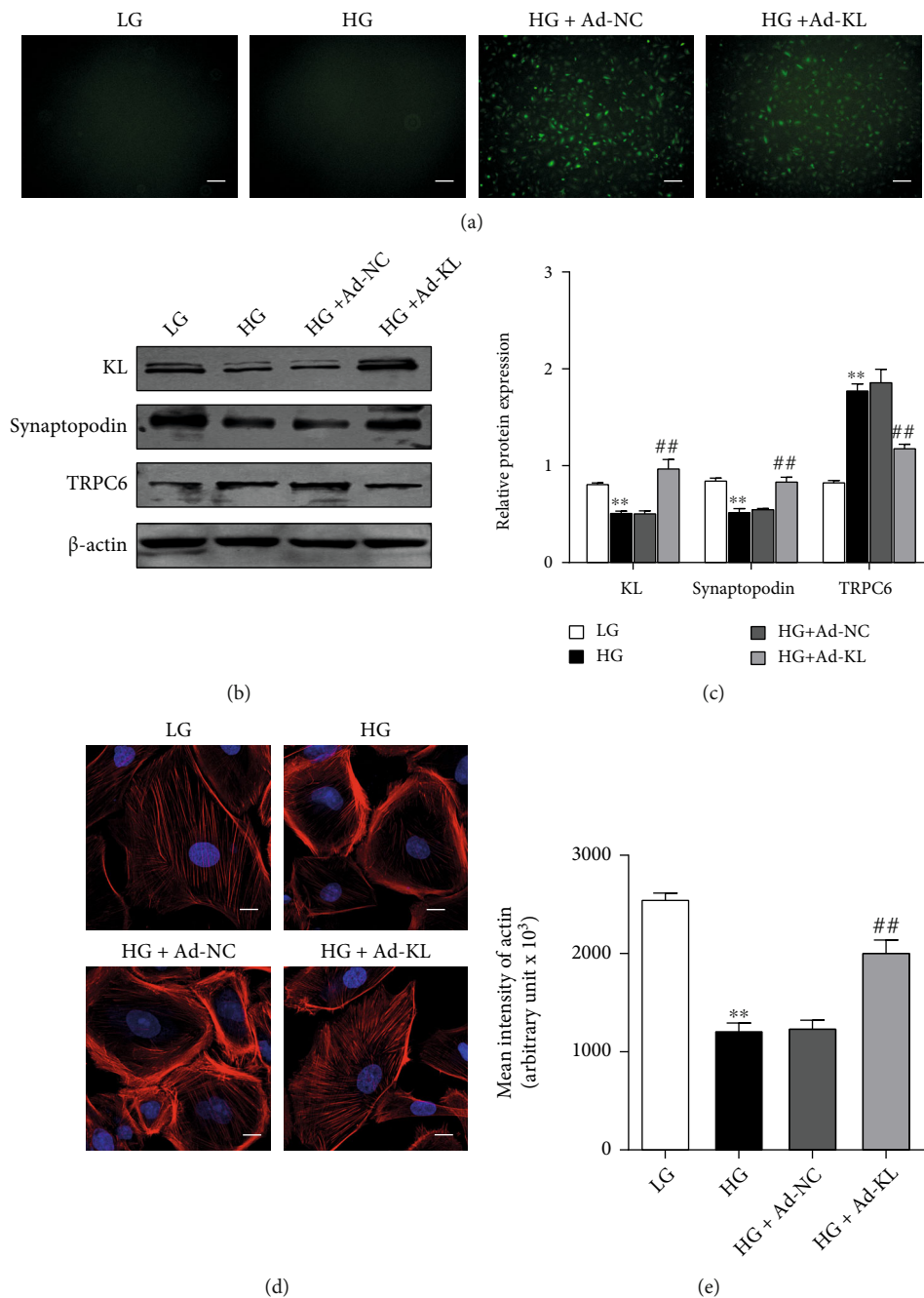


FIGURE 2: KL overexpression inhibited HG-induced podocyte injury. Podocytes were exposed to the adenovirus that expressed KL for 24 h and afterwards cultured with HG for extra 48 h. (a) The efficiency of Ad-NC and Ad-KL adenovirus infection examined by GFP fluorescence. (b) Representative western blots and (c) densitometric analyses of KL, Synaptopodin, and TRPC6 expression as aforementioned. (d) Typical images of phalloidin staining as aforementioned. Scale bars, 10  $\mu$ m. (e) Quantified outcomes in (c).  $n = 3$ . \*\* $P < 0.01$  versus LG group. ## $P < 0.01$  versus HG group.

glomerular podocytes were remarkably elevated posterior to the injection of Ad-KL with a concomitant increase in Synaptopodin expression and a marked reduction in TRPC6 expression. The *db/db* animals displayed significant albuminuria, which was significantly alleviated by Ad-KL treatment (Figure 6(d)). Compared with the *db/db* animals exposed to Ad-NC, the animals challenged with Ad-KL

showed ameliorated glomerulosclerosis, decreased podocyte foot process effacement, elevated Synaptopodin expression, and more cells positive for WT-1 in the kidneys (Figures 6(e) and 6(f)). These results indicated that KL could protect podocytes from injury and apoptosis, thereby improving glomerular filtration function and attenuating DN progression.

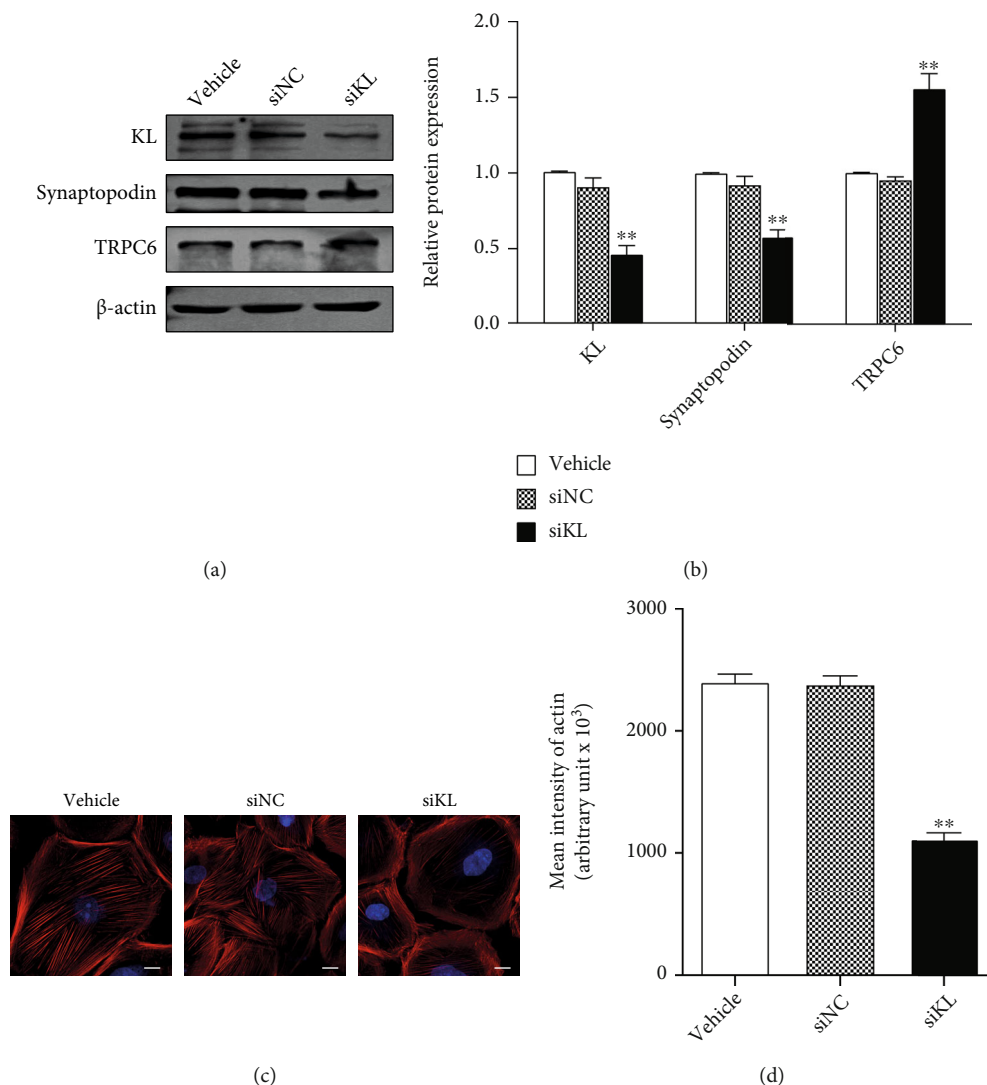


FIGURE 3: KL alleviated HG-induced podocyte injury via inhibiting TRPC6. Podocytes were exposed to the adenovirus that expressed KL for 24 h and afterwards cultured with HG for extra 48 h with or without 100  $\mu$ M FFA. (a) Typical WB and (b) densitometric analyses of TRPC6 and Synaptopodin expression as aforementioned. (c) Typical images of phalloidin staining as aforementioned. Scale bars, 10  $\mu$ m. (d) Quantification of the results in (c).  $n = 3$ . \*\* $P < 0.01$  versus LG group. ## $P < 0.01$  versus HG group. && $P < 0.01$  versus HG+Ad-KL group.

#### 4. Discussion

Podocyte damage is pivotal for the etiopathogenesis of DN. TRPC6 overexpression- or activation-evoked intracellular  $Ca^{2+}$  increase contributes to the derangement of podocyte actin cytoskeleton leading to podocyte injury and dysfunction. In this study, we found that KL could inhibit HG-induced actin cytoskeleton disruption via downregulating TRPC6, whereas the knockdown of KL resulted in podocyte actin cytoskeleton damage *in vitro*. *In vivo*, Klotho overexpression suppressed TRPC6 expression and ameliorated podocyte injury in *db/db* animals. Those outcomes revealed that KL might exert renoprotective function through inhibiting TRPC6 channel.

Podocytes are special epitheliums on the outer aspect of the glomerulus capillaries with delicate interdigitating foot processes bridged by a greatly specialised junction, the slit

diaphragm [33]. The highly dynamic foot processes contain an actin-based contractile apparatus that modulates the penetrability of the filtration barrier via variations in foot processes morphology [4]. Mutations of podocyte proteins that lead to actin cytoskeleton remodeling will disrupt the filtration barrier and result in kidney disease [33]. Therefore, the function of podocytes is largely based on their normal foot process structure, in particular on the maintenance of the actin cytoskeleton.  $Ca^{2+}$  dysregulation is pivotal for podocyte injury [34]. The elevation of  $Ca^{2+}$  in podocytes induces decomposition of Synaptopodin, an actin binding protein essential to podocyte completeness, and regulation of the Rho GTPase signal transmission which controls cytoskeleton kinetics and the morphology and migration of podocytes [34].

The TRPC pathway family comprises 7 members of nonselective  $Ca^{2+}$ -permeation pathways. Amongst them,

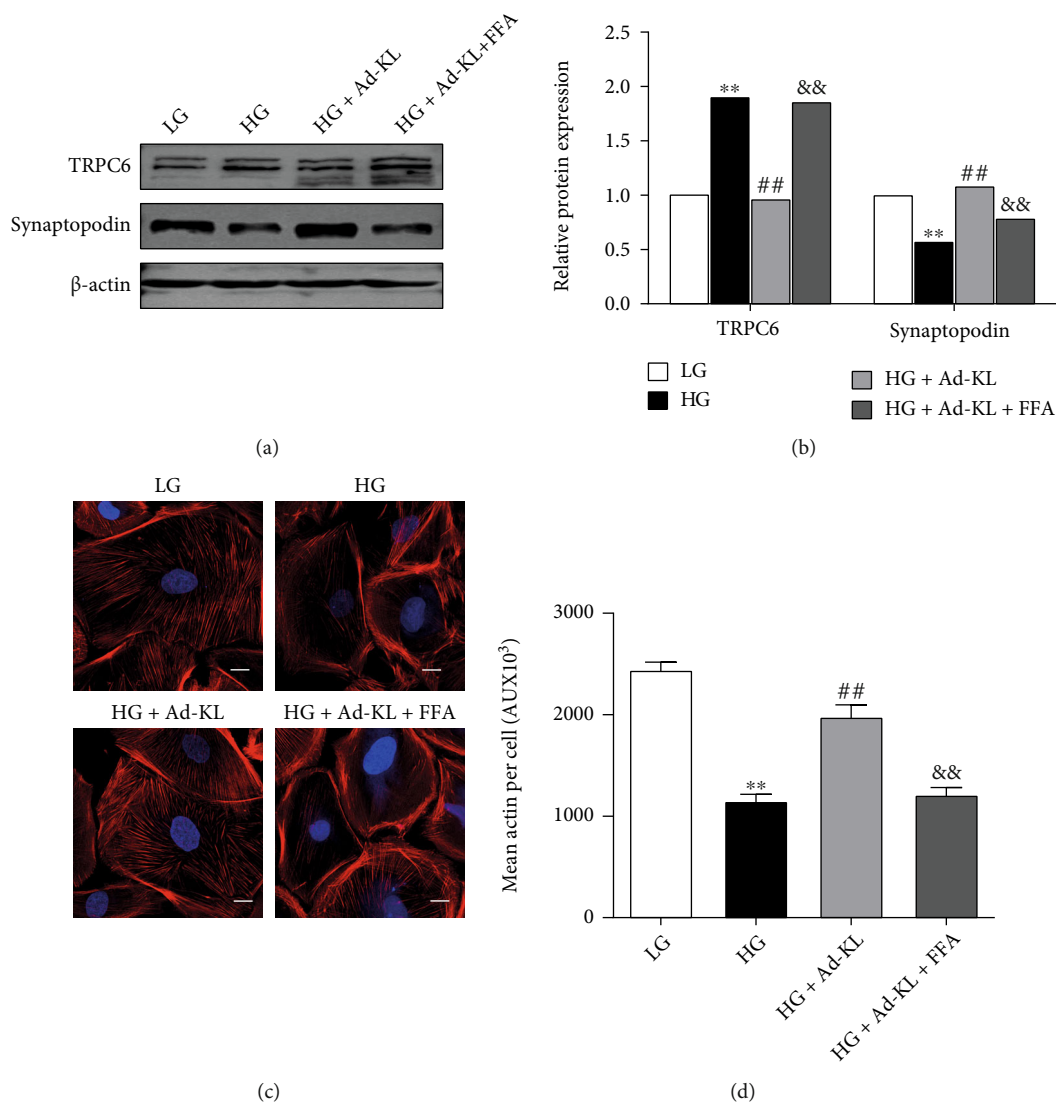


FIGURE 4: KL knockdown induced podocyte injury. (a) Typical WB and (b) densitometric analyses of KL, Synaptopodin, and TRPC6 expression in different groups. (c) Representative images of phalloidin staining in different groups. Scale bars, 10  $\mu\text{m}$ . (d) Quantification of the results in (c). Data were described as mean  $\pm$  SEM.  $n = 3$ . \*\* $P < 0.01$  versus vehicle group.

the expression of TRPC5 and TRPC6 is present in podocytes and is critical for modulating  $\text{Ca}^{2+}$  homeostasis and actin kinetics [5]. Large amount of researches have demonstrated that overactivity of TRPC5 or TRPC6 pathways induces actin cytoskeleton remodeling and albuminuria, and genetic silencing of either of them gives rise to protection [35–37]. TRPC6 is activated by hyperglycemia in renal resident cells in DN, including tubular cells, podocytes, and mesangial cells, while inhibiting TRPC6 expression or activity can delay DN progression [38–40]. Despite these findings, the upstream signaling regulating TRPC6 expression or activation has not been fully clarified.

KL is a membranous protein primarily generated in kidneys, which plays certain antiaging roles. KL deficiency has been implicated in glomerular pathophysiology [8]. A series of investigations have validated the protection potency of KL for podocytes in DN [12, 13, 41]. Nevertheless, whether and how KL directly protects podocytes are unknown. The asso-

ciation between KL and TRPC6 has been initially revealed by Xie et al. in 2012. They found that knockout of TRPC6 prevented stress-triggered heart remodeling in mice with insufficient KL [28]. Recently, another study provides evidence that KL suppressed TRPC6-mediated  $\text{Ca}^{2+}$  influx in cultured podocytes, decreased ATP-activated actin cytoskeleton rearrangement, and ameliorated TRPC6-induced albuminuria in mice [29]. KL upregulates TRPC6 via miR-30a to activate calcium/calcineurin signaling in PAN-stimulated podocytes [42]. Those discoveries revealed that TRPC6 is an underlying target of KL in podocytes in DN. Interestingly, we found that KL knockdown induced TRPC6 expression in podocytes. KL overexpression improved HG-evoked podocyte injury as demonstrated by actin cytoskeleton rearrangement and Synaptopodin downregulation and inhibited HG-induced TRPC6 expression. On the contrast, cotreatment with TRPC6 activator substantially abolished the favorable role of KL in HG-cultured podocytes. Consistently, KL

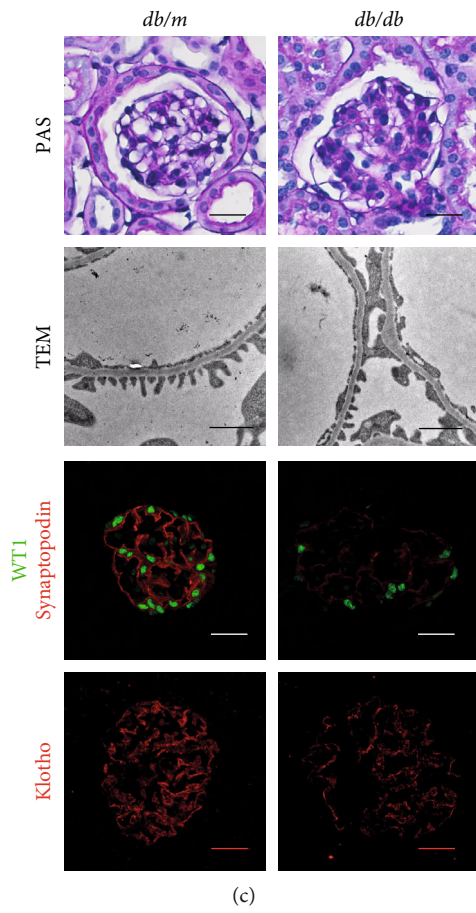
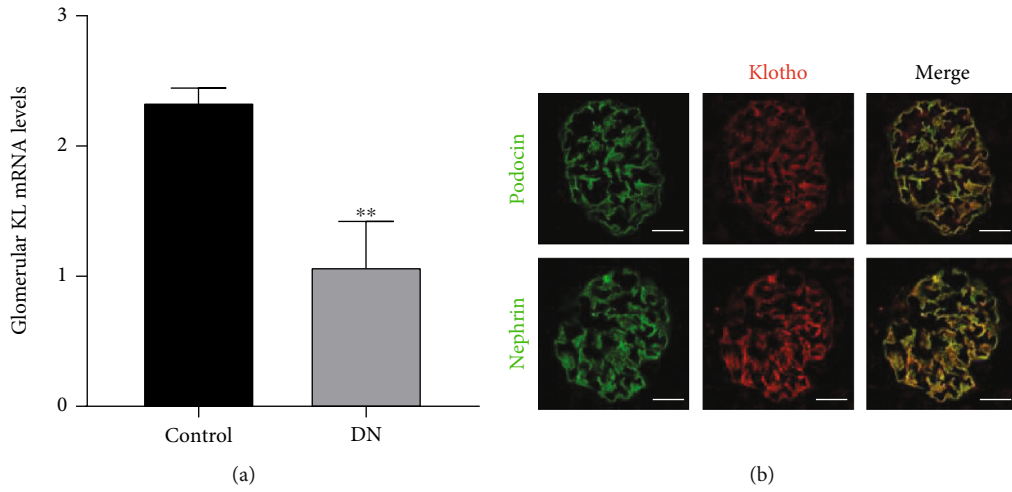
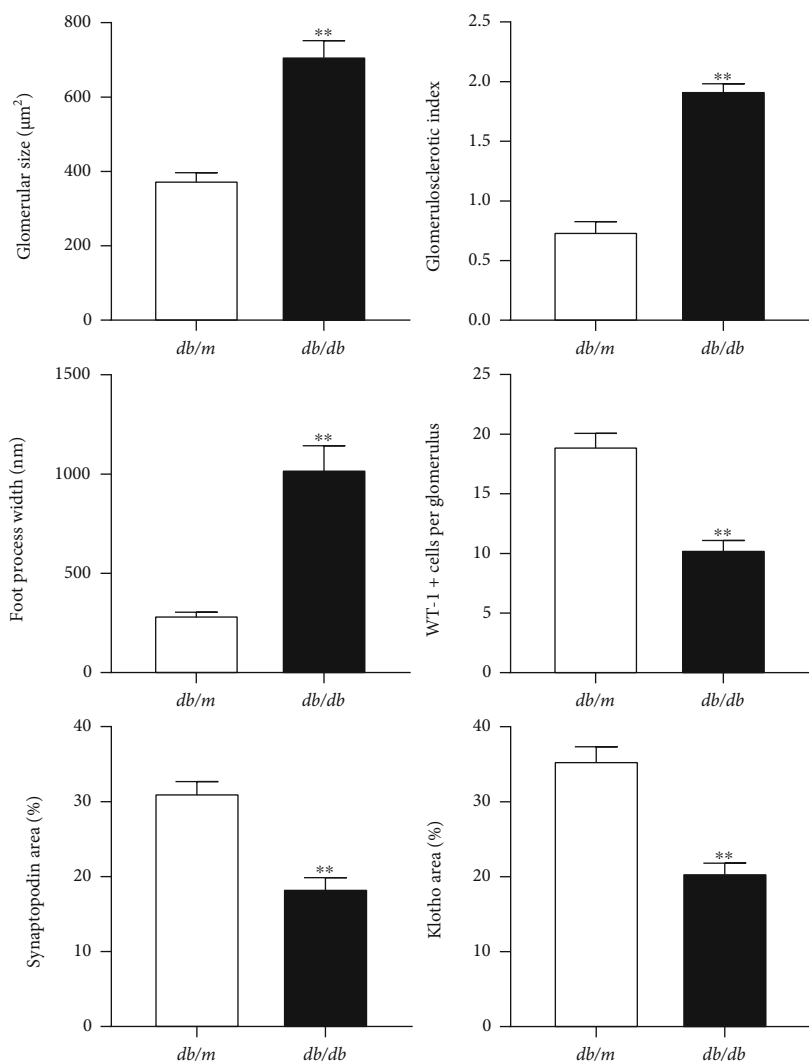
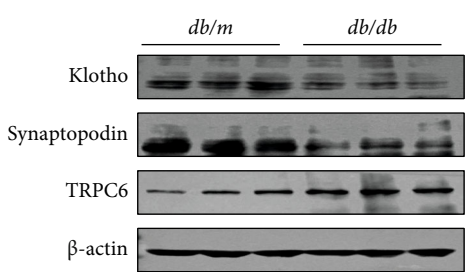


FIGURE 5: Continued.

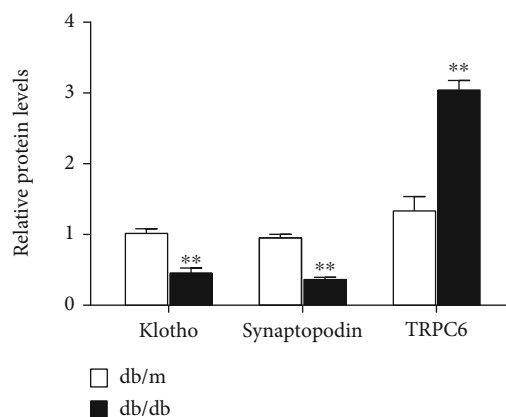




(d)



(e)



(f)

FIGURE 5: Decrease of KL expression in the glomeruli of *db/db* animals. (a) Glomerular KL expression levels in Ju CKD Glom data from Nephroseq. (b) Immunofluorescence staining unveiled that KL was colocalized with Podocin and Nephrin in podocytes. (c) Representative images of PAS, TEM, and immunofluorescence staining for WT-1, Synaptopodin, and KL in *db/m* and *db/db* animals. Scale bars for PAS, WT-1, Synaptopodin, and KL pictures, 10  $\mu\text{m}$ ; Scale bars for TEM, 10  $\mu\text{m}$ . (d) Semiquantitation of glomerular size, glomerulosclerotic index, foot process width, quantity of podocytes positive for WT-1 per glomerulus, and Synaptopodin and KL expression areas in (c). (e) Typical WB and (f) densitometric analyses of KL, Synaptopodin, and TRPC6 expression in *db/m* and *db/db* animals.  $n = 3$ . \*\* $P < 0.01$  versus *db/m* group.



FIGURE 6: Continued.

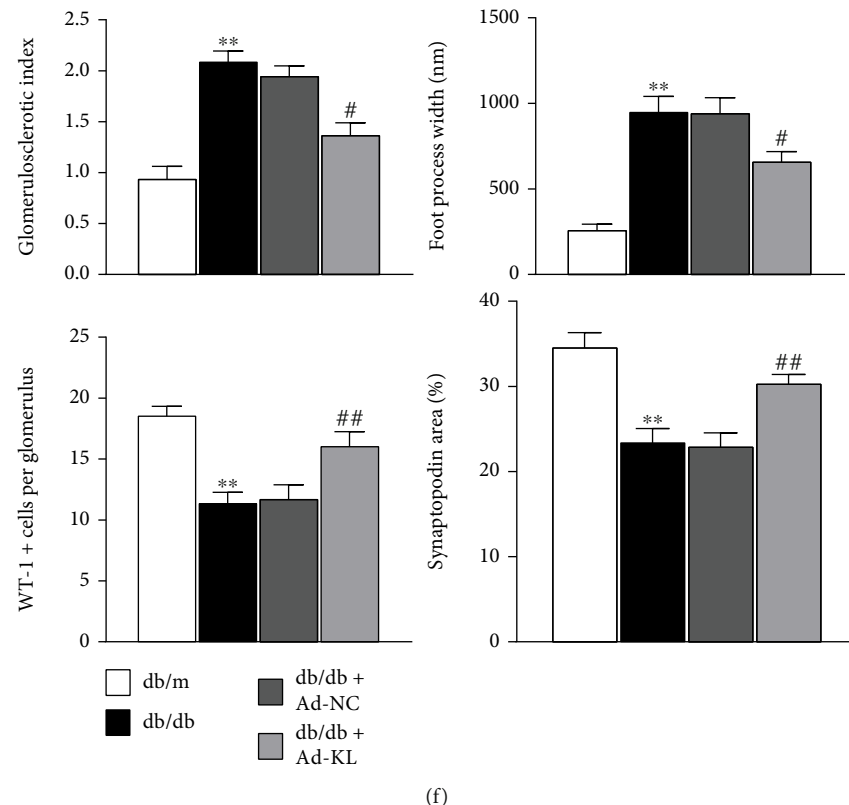


FIGURE 6: Renal KL overexpression inhibited TRPC6 and mitigated podocyte function disorder in *db/db* animals. (a) Schematic diagram of experiment process. 12-week-old *db/db* animals were inoculated with adenovirus expressing KL or negative control adenovirus via tail veins. Urine was harvested on 0 d, 7 d, 14 d, and 28 d postinjection with adenovirus, and renal samples were harvested on 28 d postinjection with adenovirus. (b) Representative western blots and (c) densitometric analyses of KL, Synaptopodin, and TRPC6 expression in the indicated groups. (d) Urinary ACR in the animals on days 0, 7, 14, and 28 postinjection with Ad-NC or Ad-KL. (e) Representative images of PAS, TEM, and immunofluorescence staining for WT-1 and Synaptopodin in the indicated groups. Scale bars for PAS staining, WT-1, and Synaptopodin pictures, 10  $\mu\text{m}$ ; Scale bars for TEM, 10  $\mu\text{m}$ . (f) Semiquantitation of glomerulosclerotic index, foot process width, quantity of podocytes positive for WT-1 per glomerulus, and Synaptopodin expression region in (e).  $n = 4-6$ . \*\* $P < 0.01$  versus *db/m* group; ## $P < 0.01$  versus *db/db* group.

overexpression improved the deteriorated renal function, the marked histopathology, and podocyte damage in *db/db* animals, with a concomitant downregulation of TRPC6. The *in vitro* and *in vivo* assays strongly suggested that KL might protect the actin cytoskeleton by inhibiting TRPC6 expression, thereby preventing podocyte injury and the progression of DN.

## 5. Conclusions

In summary, our research demonstrated that KL defended against hyperglycemia-induced podocyte injury in DN via suppressing TRPC6, which provided novel mechanistic insights for the role of KL in DN.

## Data Availability

The data used to support the findings of this study are included within the article.

## Conflicts of Interest

The authors declare that there are no conflicts of interest regarding the publication of this article.

## Authors' Contributions

Xingmei Yao, Hengjiang Guo, and Mengyao Sun contributed equally to this work.

## Acknowledgments

This work was supported by the National Natural Science Foundation of China (81903996), the Science and Technology Innovation Project of Health System in Putuo District, Shanghai (PTKWWS202104).

## References

- [1] L. Guariguata, D. R. Whiting, I. Hambleton, J. Beagley, U. Linnenkamp, and J. E. Shaw, "Global estimates of diabetes prevalence for 2013 and projections for 2035," *Diabetes*

- Research and Clinical Practice*, vol. 103, no. 2, pp. 137–149, 2014.
- [2] H. J. Anders, T. B. Huber, B. Isermann, and M. Schiffer, “CKD in diabetes: diabetic kidney disease versus nondiabetic kidney disease,” *Nature Reviews. Nephrology*, vol. 14, no. 6, pp. 361–377, 2018.
  - [3] J. S. Lin and K. Susztak, “Podocytes: the weakest link in diabetic kidney disease?,” *Current Diabetes Reports*, vol. 16, no. 5, p. 45, 2016.
  - [4] C. Faul, K. Asanuma, E. Yanagida-Asanuma, K. Kim, and P. Mundel, “Actin up: regulation of podocyte structure and function by components of the actin cytoskeleton,” *Trends in Cell Biology*, vol. 17, no. 9, pp. 428–437, 2007.
  - [5] A. Greka and P. Mundel, “Balancing calcium signals through TRPC5 and TRPC6 in podocytes,” *Journal of the American Society of Nephrology Jasn*, vol. 22, no. 11, pp. 1969–1980, 2011.
  - [6] G. I. Welsh and M. A. Saleem, “The podocyte cytoskeleton—key to a functioning glomerulus in health and disease,” *Nature Reviews. Nephrology*, vol. 8, no. 1, pp. 14–21, 2011.
  - [7] M. Kuro-o, Y. Matsumura, H. Aizawa et al., “Mutation of the mouse *klotho* gene leads to a syndrome resembling ageing,” *Nature*, vol. 390, no. 6655, pp. 45–51, 1997.
  - [8] O. M. Kuro, “The *Klotho* proteins in health and disease,” *Nature Reviews. Nephrology*, vol. 15, no. 1, pp. 27–44, 2019.
  - [9] O. Asai, K. Nakatani, T. Tanaka et al., “Decreased renal  $\alpha$ -*Klotho* expression in early diabetic nephropathy in humans and mice and its possible role in urinary calcium excretion,” *Kidney International*, vol. 81, no. 6, pp. 539–547, 2012.
  - [10] S. S. Kim, S. H. Song, I. J. Kim et al., “Decreased plasma  $\alpha$ -*Klotho* predict progression of nephropathy with type 2 diabetic patients,” *Journal of Diabetes and its Complications*, vol. 30, no. 5, pp. 887–892, 2016.
  - [11] Y. Haruna, N. Kashihara, M. Satoh et al., “Amelioration of progressive renal injury by genetic manipulation of *Klotho* gene,” *Proceedings of the National Academy of Sciences of the United States of America*, vol. 104, no. 7, pp. 2331–2336, 2007.
  - [12] Q. Wang, D. Ren, Y. Li, and G. Xu, “*Klotho* attenuates diabetic nephropathy in db/db mice and ameliorates high glucose-induced injury of human renal glomerular endothelial cells,” *Cell Cycle*, vol. 18, no. 6–7, pp. 696–707, 2019.
  - [13] L. Xing, H. Guo, S. Meng et al., “*Klotho* ameliorates diabetic nephropathy by activating Nrf 2 signaling pathway in podocytes,” *Biochemical and Biophysical Research Communications*, vol. 534, pp. 450–456, 2021.
  - [14] J. Suk Kang, S. S. Son, J. H. Lee et al., “Protective effects of *klotho* on palmitate-induced podocyte injury in diabetic nephropathy,” *PLoS One*, vol. 16, no. 4, article e0250666, 2021.
  - [15] Z. Chen, Q. Zhou, C. Liu, Y. Zeng, and S. Yuan, “*Klotho* deficiency aggravates diabetes-induced podocyte injury due to DNA damage caused by mitochondrial dysfunction,” *International Journal of Medical Sciences*, vol. 17, no. 17, pp. 2763–2772, 2020.
  - [16] A. Staruschenko, D. Spires, and O. Palygin, “Role of TRPC6 in progression of diabetic kidney disease,” *Current Hypertension Reports*, vol. 21, no. 7, p. 48, 2019.
  - [17] M. P. Winn, P. J. Conlon, K. L. Lynn et al., “A mutation in the TRPC6 cation channel causes familial focal segmental glomerulosclerosis,” *Science*, vol. 308, no. 5729, pp. 1801–1804, 2005.
  - [18] J. Reiser, K. R. Polu, C. C. Möller et al., “TRPC6 is a glomerular slit diaphragm-associated channel required for normal renal function,” *Nature Genetics*, vol. 37, no. 7, pp. 739–744, 2005.
  - [19] L. Wang, G. Jirka, P. B. Rosenberg et al., “Gq signaling causes glomerular injury by activating TRPC6,” *The Journal of Clinical Investigation*, vol. 125, no. 5, pp. 1913–1926, 2015.
  - [20] C. C. Möller, C. Wei, M. M. Altintas et al., “Induction of TRPC6 channel in acquired forms of proteinuric kidney disease,” *Journal of the American Society of Nephrology*, vol. 18, no. 1, pp. 29–36, 2007.
  - [21] X. Zhang, Z. Song, Y. Guo, and M. Zhou, “The novel role of TRPC6 in vitamin D ameliorating podocyte injury in STZ-induced diabetic rats,” *Molecular and Cellular Biochemistry*, vol. 399, no. 1–2, pp. 155–165, 2015.
  - [22] D. V. Ilatovskaya, O. Palygin, V. Chubinskiy-Nadezhdin et al., “Angiotensin II has acute effects on TRPC6 channels in podocytes of freshly isolated glomeruli,” *Kidney International*, vol. 86, no. 3, pp. 506–514, 2014.
  - [23] M. Anderson, H. Roshanravan, J. Khine, and S. E. Dryer, “Angiotensin II activation of TRPC6 channels in rat podocytes requires generation of reactive oxygen species,” *Journal of Cellular Physiology*, vol. 229, no. 4, pp. 434–442, 2014.
  - [24] E. Y. Kim, M. Anderson, and S. E. Dryer, “Insulin increases surface expression of TRPC6 channels in podocytes: role of NADPH oxidases and reactive oxygen species,” *American Journal of Physiology. Renal Physiology*, vol. 302, no. 3, pp. F298–F307, 2012.
  - [25] S. E. Dryer and J. Reiser, “TRPC6 channels and their binding partners in podocytes: role in glomerular filtration and pathophysiology,” *American Journal of Physiology. Renal Physiology*, vol. 299, no. 4, pp. F689–F701, 2010.
  - [26] D. Spires, D. V. Ilatovskaya, V. Levchenko et al., “Protective role of *Trpc 6* knockout in the progression of diabetic kidney disease,” *American Journal of Physiology. Renal Physiology*, vol. 315, no. 4, p. F1091, 2018.
  - [27] B. C. Liu, X. Song, X. Y. Lu et al., “High glucose induces podocyte apoptosis by stimulating TRPC6 via elevation of reactive oxygen species,” *Biochimica et Biophysica Acta*, vol. 1833, no. 6, pp. 1434–1442, 2013.
  - [28] J. Xie, S. K. Cha, S. W. An, M. Kuro-o, L. Birnbaumer, and C. L. Huang, “Cardioprotection by *Klotho* through downregulation of TRPC6 channels in the mouse heart,” *Nature Communications*, vol. 3, no. 1, p. 1238, 2012.
  - [29] J. H. Kim, J. Xie, K. H. Hwang et al., “*Klotho* may ameliorate proteinuria by targeting TRPC6 channels in podocytes,” *Journal of the American Society of Nephrology*, vol. 28, no. 1, pp. 140–151, 2017.
  - [30] P. Mundel, J. Reiser, A. Z. M. Borja et al., “Rearrangements of the cytoskeleton and cell contacts induce process formation during differentiation of conditionally immortalized mouse podocyte cell lines,” *Experimental Cell Research*, vol. 236, no. 1, pp. 248–258, 1997.
  - [31] S. Taneda, J. W. Pippin, E. H. Sage et al., “Amelioration of diabetic nephropathy in SPARC-null mice,” *J Am Soc Nephrol*, vol. 14, no. 4, pp. 968–980, 2003.
  - [32] Y. Zhong, K. Lee, Y. Deng et al., “Arctigenin attenuates diabetic kidney disease through the activation of PP2A in podocytes,” *Nature Communications*, vol. 10, no. 1, p. 4523, 2019.
  - [33] L. Perico, S. Conti, A. Benigni, and G. Remuzzi, “Podocyte-actin dynamics in health and disease,” *Nature Reviews. Nephrology*, vol. 12, no. 11, pp. 692–710, 2016.



- [34] A. Greka and P. Mundel, "Calcium regulates podocyte actin dynamics," *Seminars in Nephrology*, vol. 32, no. 4, pp. 319–326, 2012.
- [35] D. Q. Tian, S. M. P. Jacobo, D. Billing et al., "Antagonistic regulation of actin dynamics and cell motility by TRPC5 and TRPC6 channels," *Science Signaling*, vol. 3, no. 145, p. 77, 2010.
- [36] T. Schaldecker, S. Kim, C. Tarabanis et al., "Inhibition of the TRPC5 ion channel protects the kidney filter," *Journal of Clinical Investigation*, vol. 123, no. 12, pp. 5298–5309, 2013.
- [37] T. Nijenhuis, A. J. Sloan, J. G. J. Hoenderop et al., "Angiotensin II contributes to podocyte injury by increasing TRPC6 expression via an NFAT-mediated positive feedback signaling pathway," *American Journal of Pathology*, vol. 179, no. 4, pp. 1719–1732, 2011.
- [38] B. J. Liu, X. J. He, S. T. Li, B. Xu, L. Birnbaumer, and Y. Liao, "Deletion of diacylglycerol-responsive TRPC genes attenuates diabetic nephropathy by inhibiting activation of the TGF beta 1 signaling pathway," *American Journal of Translational Research*, vol. 9, no. 12, pp. 5619–5630, 2017.
- [39] Y. Q. Fu, C. X. Wang, D. M. Zhang et al., "Increased TRPC6 expression is associated with tubular epithelial cell proliferation and inflammation in diabetic nephropathy," *Molecular Immunology*, vol. 94, pp. 75–81, 2018.
- [40] Y. Su, Q. Chen, Y. Ju, W. Li, and W. Li, "Palmitate induces human glomerular mesangial cells fibrosis through CD36-mediated transient receptor potential canonical channel 6/ nuclear factor of activated T cell 2 activation," *Molecular and Cell Biology of Lipids*, vol. 1865, no. 12, article 158793, 2020.
- [41] W. Jiang, T. Xiao, W. Han et al., "Klotho inhibits PKC $\alpha$ /p66SHC-mediated podocyte injury in diabetic nephropathy," *Molecular and Cellular Endocrinology*, vol. 494, article 110490, 2019.
- [42] X. Qiu, J. Huo, S. Xia, W. Zhao, Y. Luo, and Y. Xia, "Dysfunction of the Klotho-mi R-30s/TRPC6 axis confers podocyte injury," *Biochemical and Biophysical Research Communications*, vol. 557, pp. 90–96, 2021.